Eur. Phys. J. A **24**, 63–67 (2005)
DOI 10.1140/epja/i2004-10129-2

THE EUROPEAN PHYSICAL JOURNAL A

Low-lying dipole strength for weakly bound systems: A simple analytic estimate

M.A. Nagarajan[1], S.M. Lenzi[2,a], and A. Vitturi[2]

[1] Department of Physics, UMIST, Manchester M60 1QD, UK
[2] Dipartimento di Fisica and INFN, Padova, Italy

Received: 16 December 2004 / Revised version: 19 January 2005 /
Published online: 1 February 2005 –
Communicated by C. Signorini

Abstract. A simple analytic expression is proposed for the total low-lying dipole strength observed in the break-up of weakly bound systems. The model assumes pure "single-particle" transitions from the "halo" weakly bound state to continuum states treated as plane waves (neutrons) or regular Coulomb functions (protons). The analytic expression for the total strength approximately depends on the inverse of the binding energy and the reduced mass of the halo, with correction factors accounting for the charge of the halo and the finite size of the potential.

PACS. 24.10.-i Nuclear reaction models and methods – 24.50.+g Direct reactions – 25.60.-t Reactions induced by unstable nuclei – 25.60.Gc Breakup and momentum distributions

1 Introduction

One of the most interesting outcomings of the experimentation with radioactive beams close to the drip lines is the observation of a strong multipole strength at the continuum threshold [1]. In particular, the break-up cross-sections are generally dominated by the low-lying dipole $B(E1)$ strength [1]. This feature is particularly useful in obtaining estimates of capture cross-sections close to the threshold, which are of relevance to astrophysical processes [2], and which cannot normally be measured directly. It is now well established that the concentration of multipole strength close to the continuum threshold is neither associated with a resonant behaviour nor is it associated with a novel collective mode [3,4]. It arises, instead, from the optimal matching of the weakly bound (and long-tailed) orbital and the low-lying continuum state in the transition matrix element. The transition matrix element derives its main contribution from the region far from the interaction radius where the bound-state wave function behaves as a simple exponential function. Under these conditions, the details of the mean field become unessential and the transition matrix element will primarily depend on the binding energy aside from the characteristics of the specific single-particle state (angular momentum and spectroscopic factor).

It is therefore tempting to obtain a simple estimate of the total low-lying dipole strength in terms of the binding energy of the system. In the following sections, we discuss the derivation of the dipole transition matrix element of radioactive nuclei with single neutron or proton halo, and compare them with more complete calculations of these elements. We shall also further comment on the modifications of these expressions for nuclei with more complicated haloes.

2 Low-lying dipole strength for a neutron halo

We will first study the case of a weakly bound one-neutron system. Within a mean-field picture, we consider the simplest case of single-particle dipole transitions from a bound neutron single-particle state $\phi_b(r)$ (with angular momentum ℓ and binding energy E_b) to a generic (ℓ'-state) $\phi_c(E_c, r)$ with continuum energy E_c. The dipole strength distribution is given by

$$\mathrm{d}B(E1)/\mathrm{d}E = (3/4\pi)(Z_{\mathrm{eff}}e)^2\langle \ell 010|\ell' 0\rangle^2 \times \left| \int \mathrm{d}r \phi_b(r)\phi_c(E_c, r) r^3 \right|^2 , \quad (1)$$

where bound and continuum states are obtained as eigenstates of the mean-field potential. In the case of a neutron dipole transition, the effective charge Z_{eff} is simply given by $-Z/A$. For simplicity the spin is neglected throughout this work. An example of the resulting dipole strength distribution is given in the inset of fig. 1 for the halo

[a] e-mail: lenzi@pd.infn.it

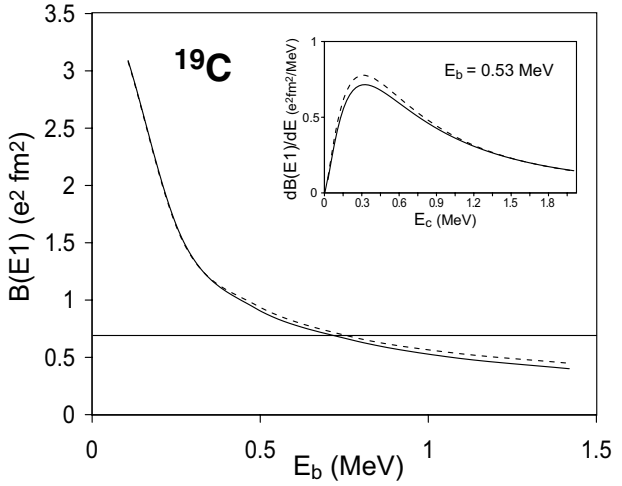

Fig. 1. Total $B(E1)$ strength in ^{19}C associated with the single-particle excitation from a bound $2s$-state to the continuum, as a function of binding energy E_b of the $2s$-state. The solid line is the "exact" calculation, where bound and continuum single-particle states have been generated from a Woods-Saxon potential, whose parameters have been adjusted to reproduce the correct binding energy of the $2s$-state. The dashed line is the prediction of the analytic expression (13). The horizontal line at 0.71 $e^2\,\mathrm{fm}^2$ corresponds to the experimental value [5]. In the inset we display the energy strength distribution as a function of the energy in the continuum, for the particular case of an initial $2s$-state bound by $E_b = 0.530$ MeV. Solid and dashed curves refer to exact and analytical results.

nucleus ^{19}C. In this case the initial $2s$ bound state and the p-wave continuum states have been generated from a Woods-Saxon potential whose depth has been adjusted to give a binding energy of 530 keV, as suggested by Nakamura *et al.* [5]. As we change this binding energy (by readjusting the mean-field potential), the strength distribution changes both in shape (the position of the maximum of the distribution approximately scales as the binding energy) and in the absolute value. The total integrated $B(E1)$ is plotted as a function of the binding energy in fig. 1, showing a clear inverse-law dependence. The model used has assumed a spectroscopic factor equal to unity for the s-wave component in the initial state. In the considered case of ^{19}C, the smaller value of the experimental $B(E1)$ (shown in the figure) with respect to the estimate value, corresponding to the assumed binding energy value of 530 keV, can be explained assuming a smaller spectroscopic factor for the s-state in the $1/2^+$ ground state.

The behaviour of the $B(E1)$ distribution can be described analytically in the limit of vanishing binding energy [6–8]. In this case, in fact, most of the contribution to the integral in expression (1) arises from the asymptotic region and therefore, for any value of r, we can treat the bound state simply in terms of its asymptotic form

$$\phi_b(r) = N_b h_\ell^{(1)}(iar), \tag{2}$$

(where $a^2 = 2\mu E_b/\hbar^2$, μ is the reduced mass of the halo neutron and N_b is the normalization) and similarly, the continuum states as plane waves normalized to a delta function in energy, namely

$$\phi_c(E_c, r) = \sqrt{\frac{2\mu k}{\hbar^2 \pi}} j_{\ell'}(kr) \tag{3}$$

($k^2 = 2\mu E_c/\hbar^2$). Under this assumption on the wave functions, the $B(E1)$ distribution gets the analytic form in terms of the binding energy E_b (via the momentum a) and the continuum energy E_c (via the momentum k):

$$\mathrm{d}B(E1)/\mathrm{d}E = \frac{3}{4\pi}(Z_{\mathrm{eff}}e)^2 \langle \ell 010 | \ell' 0\rangle^2 \times \left| \frac{2N_b k^{\ell'+1/2}}{a^{\ell'+4}} \frac{\Gamma((\ell+\ell'+4)/2)\Gamma((\ell'-\ell+3)/2)}{\Gamma(\ell'+3/2)} \times {}_2F_1\left(\frac{\ell+\ell'+4}{2}, \frac{\ell'-\ell+3}{2}, \ell'+3/2, -\frac{k^2}{a^2}\right)\right|^2 . \tag{4}$$

The strength distributions get even simpler forms in the case of transitions starting from initial s- or p-states. In the case of initial s-state the normalization N_b is equal to $\sqrt{2a^3}$ and one gets

$$\mathrm{d}B(E1)/\mathrm{d}E(s \to p) = \frac{3\hbar^2}{\pi^2\mu}(Z_{\mathrm{eff}}e)^2 \frac{\sqrt{E_b}E_c^{3/2}}{(E_c+E_b)^4} \tag{5}$$

characteristically predicting a maximum at $E_c = 3/5E_b$. Similarly in the case of initial p-state one gets dipole response functions with energy dependence

$$\mathrm{d}B(E1)/\mathrm{d}E(p \to s) = \frac{\mu}{2\pi^2\hbar^2}(\hbar^2/2\mu)^{7/2}(Z_{\mathrm{eff}}e)^2 \times N_b^2 \frac{E_c^{1/2}(E_c+3E_b)^2}{E_b^2(E_c+E_b)^4} \tag{6}$$

and

$$\mathrm{d}B(E1)/\mathrm{d}E(p \to d) = \frac{6\mu}{\pi^2\hbar^2}(\hbar^2/2\mu)^{7/2}(Z_{\mathrm{eff}}e)^2 \times N_b^2 \frac{E_c^{5/2}}{E_b^2(E_c+E_b)^4} . \tag{7}$$

As a consequence, for a dipole transition from a bound p-state the maximum of the strength occurs at $E_c = 5/3E_b$ for continuum d-states and $E_c = \frac{1}{6}(-16 + \sqrt{292})E_b \approx 0.18E_b$ for continuum s-states (see fig. 2).

We may now address the problem of the total $B(E1)$ values. The predictions of the simple model can be obtained by integrating over the continuum energy the corresponding strength distribution. A simpler procedure can, however, be used noting that, in the case of the extreme single-particle picture where the core plays a passive role and in the absence of other excited bound states contributing to the dipole transition, the total $B(E1)$ is simply related to the mean square radius of the single-particle bound-state orbital, namely

$$B(E1) = \frac{3}{4\pi}(Z_{\mathrm{eff}}e)^2 \langle r^2 \rangle. \tag{8}$$

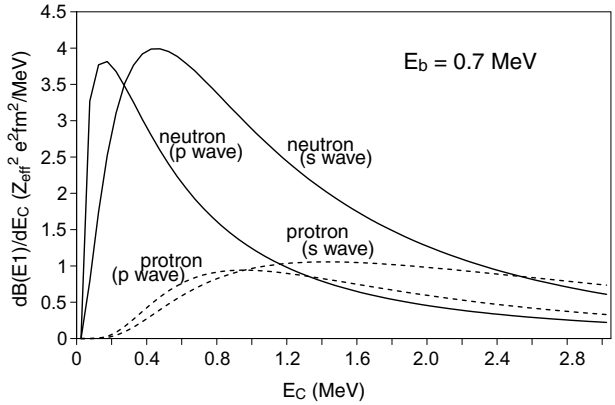

Fig. 2. $B(E1)$ strength distribution for different situations, all associated with single-particle excitation from a bound state to the continuum. In all cases the initial particle is bound with the same energy ($E_b = 0.7$ MeV). The cases labelled "neutron" refer to neutron excitations, those labelled "proton" to proton excitations. For both cases, we have considered the possibility of initial s-state (with dipole transition to p-state in the continuum) and of initial p-state (with final s-state in the continuum). Bound and continuum single-particle states have been genarated from a Woods-Saxon potential, whose parameters have been adjusted to reproduce the correct binding energy of the initial bound state.

Now, under the previous assumption on the bound-state wave function, the mean square radius for a bound s-state is simply given by

$$\langle r^2 \rangle = \frac{1}{2a^2} = \frac{\hbar^2}{4\mu E_b}, \tag{9}$$

which implies that the $B(E1)$ is inversely proportional to the binding energy,

$$B(E1) = \frac{3\hbar^2}{16\pi}(Z_{\rm eff}e)^2 \frac{1}{\mu E_b}. \tag{10}$$

In actual cases, one expects deviations from the simple law, due to the effect of the binding potential on the bound wave function both in the internal (deviation from the exponential behaviour) and in the external region (different normalization). An expression for this correction can be obtained assuming a square-well potential of radius R. It is possible to show that in that case the mean square radius can be obtained as

$$\langle r^2 \rangle = \frac{2a^3R^3 + 6a^2R^2 + 6aR + 3}{6a^2(1+aR)} = \frac{1}{2a^2}F(E_b, R), \tag{11}$$

where

$$F(E_b, R) = \frac{2a^3R^3 + 6a^2R^2 + 6aR + 3}{3(1+aR)} \approx 1 + aR + a^2R^2. \tag{12}$$

Consequently, the $B(E1)$ assumes the same expression as before, but with a correction factor, namely

$$B(E1) = \frac{3\hbar^2}{16\pi}(Z_{\rm eff}e)^2 \frac{1}{\mu E_b} F(E_b, R)\,. \tag{13}$$

It may be reasonable to assume that the same multiplicative correction factor, that depends on the binding energy and on the radius R, can be applied to the energy strength distribution (eq. (5)), even if the introduction of a finite potential leads to some redistribution of the strength. In the case of other mean fields (*i.e.* different from the square well) the expression becomes only approximated. In the particular case of a Woods-Saxon potential, the equivalent square-well radius should be larger than that of the Woods-Saxon potential because of the diffuseness of the latter. A rough estimate indicates a value of $R = R_{\rm WS} + 3d$, d being the diffusivity of the potential (typically $d = 0.6$ fm).

The $B(E1)$ values obtained with the analytic expression are compared in fig. 1 with the exact values. As apparent from the figure, there is a very good agreement, even for relatively large binding energies (of the order of 1–2 MeV). Similar agreement is obtained for the energy strength distribution, as shown in the inset. To get an idea of the effect of the correction factor (12), its value is about 2 for $E_b = 0.7$ MeV, reducing to a 10% correction only for binding energies less than 10 keV.

3 The case of charged haloes

The previous picture has inevitably to be modified in the case of charged haloes. In this case, in fact, aside from the different expression for the effective charge $Z_{\rm eff} = N/A$, we expect *ceteris paribus* a reduction of the $B(E1)$ as a consequence of the confining effect on the bound-state wave function originating from the Coulomb barrier. To give an idea of the effect, we compare in fig. 2 the $B(E1)$ energy distributions for one-proton and one-neutron haloes, taking the same value of the binding energy. We have considered both the cases of s and p initial value of the orbital angular momentum. For the sake of comparison, to avoid the variation of other parameters we have considered in both cases an ideal (although unrealistic) system with mass $A = 8$ and a nucleon binding energy $E_b = 0.7$ MeV. In the case of a proton halo, the strength distribution is shifted to higher energies, together with a damping of the absolute value.

In order to obtain analytic expressions for the response function also in the case of charged haloes, we adopt the model of Bhagwat *et al.* [9] where the asymptotic form of the proton wave function (in the case of s-wave) is approximated by

$$\psi_b(r) = N_0 \frac{e^{-ar}}{(ar)^\alpha}, \tag{14}$$

where a is defined as before in terms of the binding energy E_b, while α is dependent on the Coulomb potential and is defined as

$$\alpha = 1 + \frac{\mu q Q e^2}{\hbar^2 a}, \tag{15}$$

$q = 1$ being the charge of the proton and $Q = (Z-1)$ the charge of the core. The parameter α is thus different from unity by a large amount as one passes to very

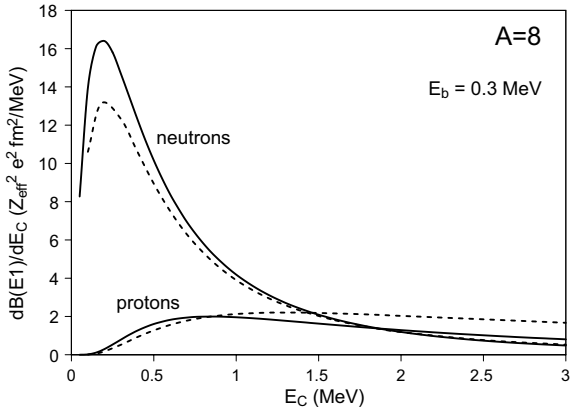

Fig. 3. $B(E1)$ strength distribution associated with the single-particle neutron and proton excitation from a bound s-state to the continuum. We have chosen a binding energy $E_b = 0.3$ MeV for the s-state. The solid line is the "exact" calculation, where bound and continuum single-particle states have been generated from a Woods-Saxon potential. The dashed line is the prediction of the analytic expressions (5) and (18), respectively.

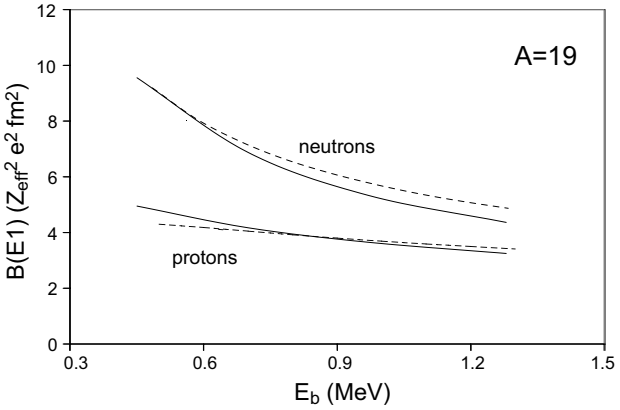

Fig. 4. Total $B(E1)$ strength associated with the single-particle excitation from a bound s-state to the continuum, as a function of binding energy E_b of the s-state. Both proton and neutron cases are shown. The solid lines are the "exact" calculations, where bound and continuum single-particle states have been generated from a Woods-Saxon potential (modelled to simulate the ^{19}C nucleus in the neutron case), whose depth has been adjusted to reproduce the correct binding energy of the s-state. The dashed lines are the predictions of the analytic expressions (13) and (20) for the neutron and proton cases, respectively.

weakly bound systems. To give a simple estimate we assume, however, the normalization constant N_0 to be still equal to $(2a^3)^{1/2}$. Similarly, for the continuum wave function we can assume

$$\psi(E_c, r) = \sqrt{\frac{2\mu k}{\hbar^2 \pi}} \frac{F_\ell(kr, \eta)}{kr} \tag{16}$$

in terms of the regular Coulomb function $F_\ell(kr, \eta)$, $\eta = (Z-1)\mu e^2/(\hbar^2 k)$ being the Sommerfeld parameter. Under these assumptions the dipole matrix element from the bound s-state to the continuum p-state entering in the $B(E1)$ distribution

$$\mathrm{d}B(E1)/\mathrm{d}E = \frac{3}{4\pi}(Z_{\mathrm{eff}}e)^2 |M_{s\to p}(E1, E_b, E_c)|^2 \tag{17}$$

is analytically given by

$$\begin{aligned} M_{s\to p}(E1, E_b, E_c) = & \int_0^\infty \psi_b(r)\psi(E_c, r) r^3 \mathrm{d}r = \left(\frac{4\mu a^3}{\hbar^2 \pi}\right)^{1/2} \\ & \times \frac{k^{3/2}\Gamma(2+i\eta)\Gamma(5-\alpha)}{3\ a^\alpha (a+ik)^{5-\alpha}\ e^{\pi\eta/2}} \\ & \times {}_2F_1\left(5-\alpha, 2-i\eta, 4, \frac{2ik}{a+ik}\right). \end{aligned} \tag{18}$$

A comparison of the analytic expression with the exact calculation is performed in fig. 3 for an ideal system of mass $A = 8$ and a single-particle halo in a s-state bound by 0.3 MeV. As the figure shows, the approximated formulae satisfactorily reproduce the exact trend, with both the shift to higher energies and the reduction in magnitude.

Similar arguments can be carried on for the total $B(E1)$. As discussed in the previous section, under the hypothesis of a single-particle excitation and in the absence of the other bound excited state, the total $B(E1)$ can be directly obtained from the mean square radius of the weakly bound proton. In the case of a s-state, using the asymptotic expression only beyond a certain value of r and using for smaller values the wave function as that in a square well, we obtain

$$\langle r^2 \rangle_p = \frac{(2aR)^3 e^{-2aR} + 6(2aR)^{2\alpha-2}\Gamma(5-2\alpha, 2aR)}{12a^2(2aRe^{-2aR} + 2(2aR)^{2\alpha-2}\Gamma(3-2\alpha, 2aR))} \tag{19}$$

in terms of the incomplete Gamma function. Note that for $\alpha = 1$ (neutral case), this expression reduces to the previous expression (11). Consequently, the total $B(E1)$ strength assumes the form

$$\begin{aligned} B(E1) = & \frac{3\hbar^2}{16\pi}(Z_{\mathrm{eff}}e)^2 \frac{1}{\mu E_b} \\ & \times \frac{((2aR)^3 e^{-2aR} + 6(2aR)^{2\alpha-2}\Gamma(5-2\alpha, 2aR))}{6(2aRe^{-2aR} + 2(2aR)^{2\alpha-2}\Gamma(3-2\alpha, 2aR))}. \end{aligned} \tag{20}$$

A comparison of the analytic expressions (13) and (20) with the exact calculations are shown for both neutrons and protons in fig. 4. It can be seen that, at variance with the neutron case, where the $B(E1)$ increases dramatically as one proceeds to very low binding energy, the change for protons is very gradual, indicating that the dominant effect is due to the Coulomb interaction that damps the wave function severely in the asymptotic region.

4 Summary and conclusions

We have shown that, under the simplifying assumption that the main contribution to the dipole transition matrix elements arise from regions outside the interaction radius,

a simple analytic expression can be obtained for both neutron and proton halo nuclei (a similar expression has also been recently proposed by Forssén *et al.* [10]). Allowing for corrections due to the effect of the binding potential, the total $B(E1)$ for a neutron halo nucleus is shown to be inversely proportional to its binding energy, becoming very large for nuclei with very small binding energies. In contrast, in the case of a proton halo nucleus the total $B(E1)$ still depends on the binding energy but the dominant effect arising from the Coulomb interaction results in a very gradual increase in its value as one proceeds to nuclei with very small binding energy. Furthermore, the Coulomb effect shifts the energy distribution of the dipole strength to higher continuum threshold and diminishes its magnitude, compared with that of a neutron halo nucleus.

The arguments developed in the previous sections refer to the case of a system characterized by a single-nucleon halo. The same argument can be advanced for multi-nucleon haloes, treated in the cluster model. If system (A, Z) is described in terms of a core $(A - A_c, Z - Z_c)$ and a halo of mass A_c, bound with binding energy E_b, all previous expressions will still hold, with proper values of the reduced mass $\mu = (A - A_c)A_c/A$ and of the effective charge $Z_{\rm eff} = -ZA_c/A$ for a neutral halo, and $Z_{\rm eff} = (Z_c(A - A_c)/A) - ((Z - Z_c)A_c/A)$ for a halo with charge Z_c. Simply the initial and final single-particle states have to be replaced by the initial and final states describing the relative motion of the two clusters. Dipole transitions will promote the cluster relative motion into a dipole state with energy in the continuum. An example of this situation might be provided by the nucleus ^{7}Li, treated as an alpha plus a triton system [11].

The simple estimates for the total break-up cross-sections (or the total $B(E1)$) could be used to predict capture cross-sections for the inverse processes of relevance to astrophysics. The $1/E_b$ law suggests the possibility of making a systematics of all available $B(E1)$ data. They should in fact be distributed on a unique universal curve if plotted against the binding energy. To put on the same footing one-nucleon and cluster haloes, due to the variation in the reduced mass and effective charge, when comparing different systems one should compare the total $B(E1)$ not directly with E_b, but rather with $\mu E_b/(Z_{\rm eff}\ e)^2$: the $B(E1)$ should approximately depend inversely on $\mu E_b/(Z_{\rm eff}\ e)^2$. Our results differ from the phenomenological systematics recently advanced by Kolata [12] for the total break-up reaction (and consequently for the total $B(E1)$ strength within the model of treating break-up processes as transitions to the continuum), where a correlation is made between the total cross-section and the neutron separation energy (which would be different from the binding energy in the case of charged or cluster haloes).

References

1. A. Bracco, P.F. Bortignon (Editors), *Proceedings of the Giant Resonances Conference, Varenna, Italy, 11-16 May 1998*, Nucl. Phys. A **649** (1999); T. Wasaka, M. Fujiwara, M. Nomachi, H. Ejiri (Editors), *Proceedings of the GR2000 Conference, Osaka*, Nucl. Phys. A **687** (2001).
2. K. Langanke, M. Wiescher, Rep. Prog. Phys. **64**, 1657 (2001).
3. F. Catara, C.H. Dasso, A. Vitturi, Nucl. Phys. A **602**, 181 (1996).
4. I. Hamamoto, H. Sagawa, X.Z. Zhang, Phys. Rev. C **53**, 765 (1996); I. Hamamoto, H. Sagawa, Phys. Rev. C **53**, R1492 (1996); I. Hamamoto, H. Sagawa, X.Z. Zhang, Phys. Rev. C **57**, R1064 (1998).
5. T. Nakamura *et al.*, Phys. Rev. Lett. **83**, 1112 (1999).
6. C.A. Bertulani, G. Baur, Nucl. Phys. A **480**, 615 (1988).
7. T. Otsuka, M. Ishihara, N. Fukunishi, T. Nakamura, M. Yokoyama, Phys. Rev. C **49**, R2289 (1994).
8. D.M. Kalassa, G. Baur, J. Phys. G **22**, 115 (1996).
9. A. Bhagwat, Y.K. Gambhir, S.H. Patil, Eur. Phys. J. A **8**, 511 (2000).
10. C. Forssén, N.B. Shul'gina, M.V. Zhukov, Phys. Lett. B **549**, 79 (2002).
11. L. Fortunato, A. Vitturi, Nucl. Phys. A **722**, 85c (2003).
12. J.J. Kolata, Phys. Rev. C **63**, 061604(R) (2001).